

## Theoretical Approach to Study Assembly Nature of Molecular Modeling System of Carbon Nanotube and a Nematic Liquid Crystal

Alaa Adnan Rashad\*, Nasreen Raheem Jber and Mehdi Salih Shihab  
Department of Chemistry, College of Science, Al-Nahrain University, Baghdad-Iraq.  
E-mail\*: alaache\_2011@yahoo.com.

### Abstract

Theoretical study for stable geometries of a nematic liquid crystal (LC) molecule assembled on the carbon nanotubes (CNT) wall by using semi-empirical molecular quantum calculations within the PM3 method as implemented in Hyperchem package. The interaction influence of  $\pi,\pi$ -stacking between N-4'-Methoxybenzylidene-4-n-butylaniline (MBBA) liquid crystal molecule on the CNT wall led to formation of the local short range orientation order by LC molecules on the surface of the CNT due to the LC-CNT binding energy ( $\pi,\pi$ -stacking). The binding energy of the LC molecule on the CNT wall was within the typical van der Waals interaction. This binding originated from the electrostatic energy by a significant amount of charge transfer from the LC molecule to the CNT.

Keyword: Liquid crystal, Carbon nanotube, N-4'-Methoxybenzylidene-4-n-butylaniline (MBBA).

### Introduction

Electronic structure methods provide useful information on the molecular structure and charge distribution, so they are useful to understand and describe systems where electronic effects and molecular orbital interactions are dominant. Depending on the theoretical assumptions used for calculations, electronic structural methods belong to one of two fundamental groups: ab initio and semi-empirical.

In particular, the semi-empirical PM3 method makes use of an accurate procedure to predict chemical properties, through a simplified Hartree-Fock (HF) Hamiltonian [1]. It is the nature and strength of various types of intermolecular interactions acting between sides, planes and ends of a pair of molecules, which are solely responsible for the liquid crystalline behavior of molecules. Using computer simulation and theoretical methods efforts have been made by several researchers to understand the role of molecular interactions in liquid crystalline [2-4]. It has been observed that the pair potential between such molecules is anisotropic in nature, which is in general regarded as prime requirement for the mesophase formation in thermotropic liquid crystals. Theoretical study of molecular ordering in p-n-hexyloxybenzylidene-p-toluidine (a nematic liquid crystal) is used to elucidate the

nematogenic behavior [5]. The electronic structure method at the ab initio HF/3-21G//PM3 level has been used to study the observed liquid crystal behavior of a 4'-alkyl-biphenyl-4-carbonitrile and 4'-alkoxy-biphenyl-4-carbonitrile homologous-series, this quantum-mechanical methodology computed a number of molecular properties (like, ovality, electric quadrupolar moment and the anisotropy) that used to correlate to the experimental mesomorphic behavior of the chosen molecules [6]. The structural study by AM1 semi-empirical calculation was described for liquid crystalline of a new series of amides incorporating pyridine and 1, 3, 4-thiadiazole rings [7].

Molecular parameters, such as the polarizability and its anisotropy, the dipole moment and its angle with the molecular long axis, were taken from semi-empirical quantum chemistry (MOPAC/AM1) modeling of nematic liquid crystals [8]. Semi empirical quantum calculations and experimental data show that the difference of the dielectric anisotropy value is influenced by the difference of the dipole moment value and the direction of the dipole at the most stable conformation for a series of novel liquid crystalline compounds with a tetrahydropyran ring [9].

It has been reported that a minute addition of carbon nanosolids such as fullerene and

multiwall carbon nanotubes dispersed in a twisted nematic LC affects the electro-optical properties of the (nematic liquid crystal–carbon nanotubes) cell. Among them are the threshold voltage, response time, and residual DC [10, 11].

It has been demonstrated that inside a nematic liquid crystal matrix, the long axes of carbon nanotubes (CNTs) orient parallel to the director field (average direction of LC molecules) with an orientational order parameter  $S$  between 0.6 – 0.9 [12,13], while bulk nematic liquid crystals themselves have orientational order of  $S \approx 0.6$ . Recent theoretical work shows that a strong interaction between LC and CNT is mainly due to surface anchoring with a binding energy of about  $-2$  eV for  $\pi,\pi$ -stacking which is associated with the CNT alignment mechanism in the nematic state [14,15]. This anchoring energy induces local short-range orientation order of LC molecules surrounding the CNT-wall having local director along the tube axis, shown schematically in Fig. (1).

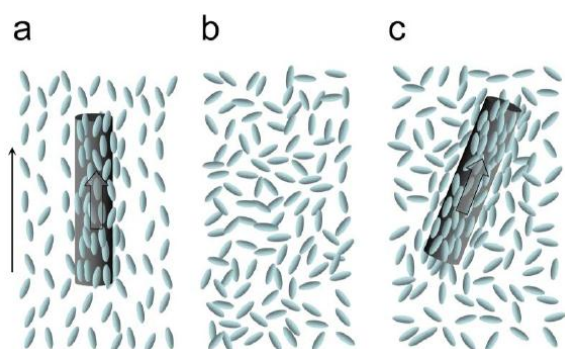


**Fig.(1) Schematic diagrams; (a) the presence of a CNT (cylindrical) in a nematic LC media; and formation of the local short range orientational order by LC molecules on the surface of the CNT due to the LC-CNT anchoring energy ( $\pi,\pi$ -stacking). The thin arrow represents the long-range nematic director and the thick arrow on the CNT represents the short range local director (b) the isotropic phase of LC; (c) the presence of a CNT (cylindrical) in an isotropic LC media and formation of the local short range orientational order by LC molecules [16].**

The mean induced short-range orientation order increases the net polarizability of the system. In the nematic matrix, a CNT long

axis is coupled to the nematic director [17] and, so, the nematic state gains an additional orientational order for this anchoring energy due to the presence of CNTs. Thus, one can visualize the suspended CNTs in the nematic media as local anchoring fields along the nematic director that amplify the orientational order in the matrix. This enhancement in orientational order causes an increase in dielectric anisotropy ( $\Delta\epsilon$ ) in the hybrid system.

### Theoretical Methods

The total energy calculations and corresponding structure optimizations of the most stable geometries were based on semi-empirical molecular quantum calculations within the PM3 method and molecular mechanics within MM+ level as implemented in Hyperchem package version 7.52 [18]. No frozen core approximation was used throughout the calculations. All calculations were carried out in gas phase and  $25^\circ\text{C}$ .

The binding (or adsorption) energy ( $E_{\text{ad}}$ ) of the LC molecule on the CNT wall was defined as:

$$E_{\text{ad}} = E_{\text{t}}(\text{CNT-LC}) - E_{\text{t}}(\text{CNT}) - E_{\text{t}}(\text{LC})$$

Where  $E_{\text{t}}$  is the total energy of a given system. A typical imine LC molecule, N-4'-Methoxybenzylidene-4-n-butylaniline (MBBA) has been chosen for the model calculation. This molecule is composed of several parts, two hexagonal rings with methoxy fragment head part and an alkyl chain tail part, one azomethane fragment as mesogenic group. The head part contained polar terminal group and mainly determined the dielectric anisotropy ( $\Delta\epsilon$ ) of the LC molecule.

We chose a (10, 0) zigzag CNT with the CNT length of 9 layers with  $20 \text{ \AA}$  long along the tube axis and  $8 \text{ \AA}$  diameters. This was presumably short compared to the experimentally used one but at least longer than the LC length ( $16 \text{ \AA}$ ) such that the interaction between the CNT and LC molecule was fully incorporated in the model calculation. We considered one case of CNTs: Open nanotube, hydrogen-terminated nanotubes.

## Utilized Computer

HyperChem was run with Pentium (R) dual CPU T2330 computer under some of these operating systems:

- 1- Microsoft windows XP.
- 2- Hard disc : 250 Gb.
- 3- CPU : 1.6 GHz.
- 4- CD Ram : 1 Gb .

## Results and Discussion

### A. The Stable Geometry of the MBBA Molecule

We first searched for the stable MBBA geometry from the chemical structure. The MBBA molecule had one nitrogen and oxygen atoms in the whole structure of MBBA molecule. The computed charges of nitrogen atom (-0.061 e/atom), oxygen atom (-0.186 e/atom) and the average charge of the carbon atoms in two rings (-0.100 e/atom) were negatively charged. The charges which extracted from hydrogen atoms are about (+0.110 e/atom) in the rings and about (+0.040 e/atom) in the chain tail group. These charges of the molecules were determined from the Mulliken charge population.

This difference in charge transfer leads to the creation of a significant dielectric constant. The conformational structure of MBBA molecule in the mesogenic model (we suggest head and tail terms), as shown in the Fig. (2).

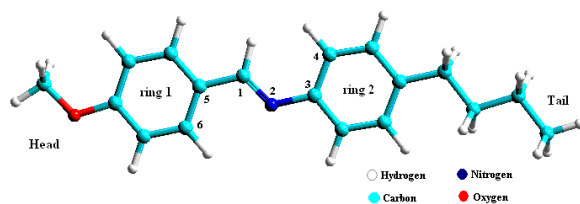


**Fig.(2) Conformation final structure of the MBBA molecule.**

The total energies were calculated after the geometries were fully relaxed. The most stable geometry for the MBBA was a flat conformation (related to imine group with two rings) as depicted in Fig. (2). It is well known that the flat conformation is more stable for this kind of compound [19]. With flat structure the dihedral angles, ( $C_1-N_2-C_3-C_4$  and  $N_2-C_1-C_5-C_6$ ) are equal to zero (related to imine group with two rings). Thus, it has a minimum angle strain and torsional strain. This flat

geometry was used in the subsequent calculations for the interaction between the CNT and LC molecule.

### B. Interaction between the MBBA Molecules

We describe here the types of interactions between two MBBA molecules. Fig.(3) shows the interaction between two molecules parallel to each other, as denoted for the head-head (H-H) type shown in model (A) and anti parallel for the head-tail (H-T) type shown in model (B). Here the H-H type result in higher heat of formation than the (H-T) type through calculation method of PM3, favoring the H-T interaction, see Table (1). This explains why the nematic LC medium does not possess a permanent dipole moment despite the fact that the individual LC molecule has a permanent dipole moment [20].

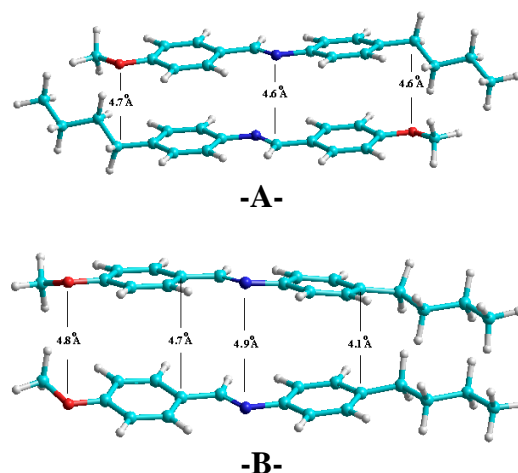


**Fig.(3) Interaction groups of two LC molecules.**

The distance between two MBBA molecules is depicted in the Fig. (3). The shortest distance between two LC molecules was about 4 Å longer than the general van der Waals interaction distance [21]. The binding energy was dependent on the basis set level of calculations and types of correlation energy, and shows the H-T type was the most stable geometry. Because of the fluctuation of electron density was effected on electrostatic interaction was dominant by van der Waals interaction (see Table (1)).

Fig. (4) shows electrostatic potential energy maps (or molecular electrical potential surfaces) of MBBA molecule, H-T MBBA model and H-H MBBA model which are electrostatic potential energy in which the

charge distribution within the range (-0.09 to +0.59 in unit  $e/\text{atom}$ ), illustrate the charge distributions of molecules three dimensionally. These maps allow us to visualize variably charged regions of a molecule. Knowledge of the charge distributions can be used to determine how molecules interact with one another.

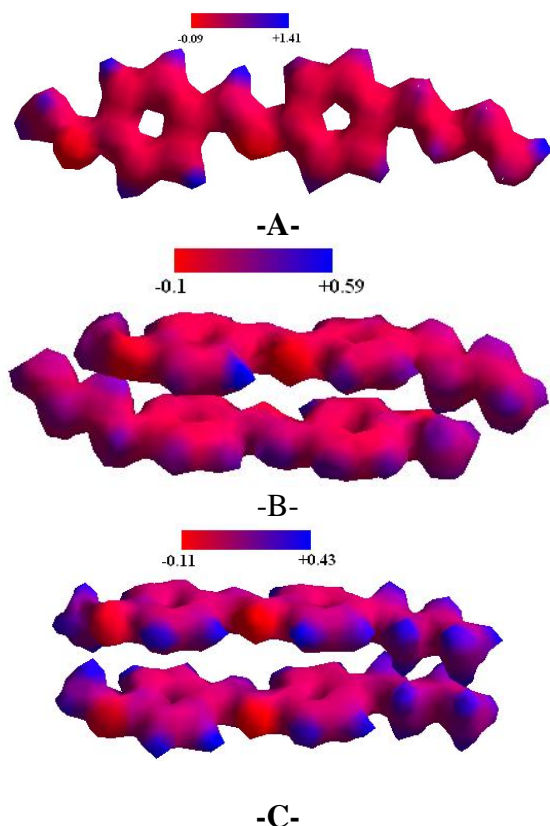


**Fig. (4) Electrostatic potential maps of:**  
A) MBBA molecule, B) H-T MBBA model,  
C) H-H MBBA model.

### C. Interaction between the MBBA Molecule and CNT

Fig. (5) presents two different views of nanotube that has an open nanotube (10,0) with hydrogen-terminated nanotube. Fig. (6) show some of C-C bonds length of part of hydrogen terminated open CNT (10, 0). In addition to representing the open nanotube, the termination of dangling bonds provided less strain to the carbon atoms near the edge, making them ideal structures. It also enhanced the computational speed by using Molecular Mechanics method for primary optimization then followed by semi-empirical PM3 method as final optimization.

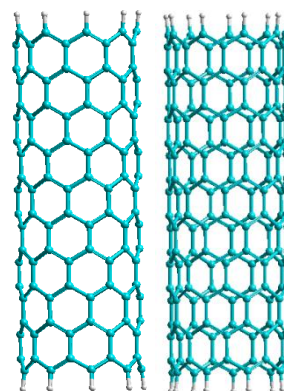


**Fig. (5) CNT geometries for open (10, 0) hydrogen-terminated nanotube.**

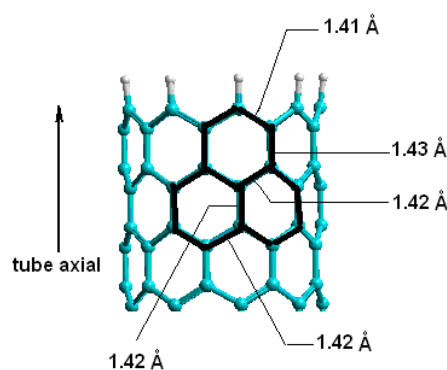


**Fig.(6) Part of hydrogen terminated open CNT (10,0) shown some of C-C bonds length.**

Fig. (7) shows the electrostatic potential energy maps of CNT system that illustrates electronic density distribution over the surface area of CNT molecule.

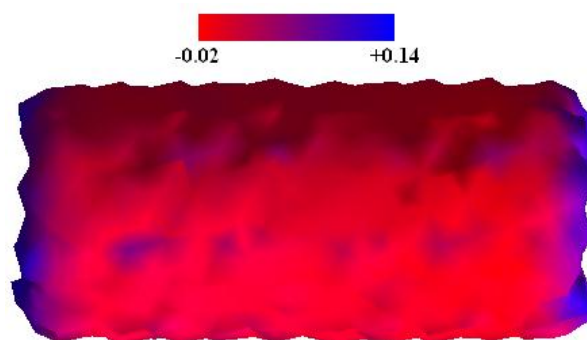


**Fig. (7) The electrostatic potential map of CNT system.**

We also defined an assembly of the MBBA molecule on the CNT surface, as shown in Fig. (8) that describes the interaction between MBBA molecule and CNT molecule. It is clear from the Fig. (8) that MBBA

molecule has different conformation comparing with Fig.(1); especially the dihedral angle ( $C_1-N_2-C_3-C_4$ ) has  $22^\circ$  and curvature shape around CNT molecule. In addition, the difference among frontier orbital energies among assembly MBBA-CNT model and components indicate for interaction between MBBA molecule and CNT molecule (see Table (1)).

We observed that the interaction was strengthened by the  $\pi,\pi$ -stacking through the hexagonal rings in the MBBA molecule and the CNT wall that are confirmed by the changing of variation of the charge of aromatic carbons rings in MBBA,, as shown in Table (2). This explains the experimental observations that the ring-type molecule was dominated by  $\pi,\pi$ -stacking with the CNT wall [22]. We believe that the difference in distribution of electronic density and energy levels (HOMO and LUMO, (see Table (1)) in both MBBA and CNT molecules prepare proper conditions for interaction. As a consequence, the separation distances between atoms of MBBA molecules and carbon atoms in CNT were within the typical van der Waals interaction distance, as shown in Fig.(8).

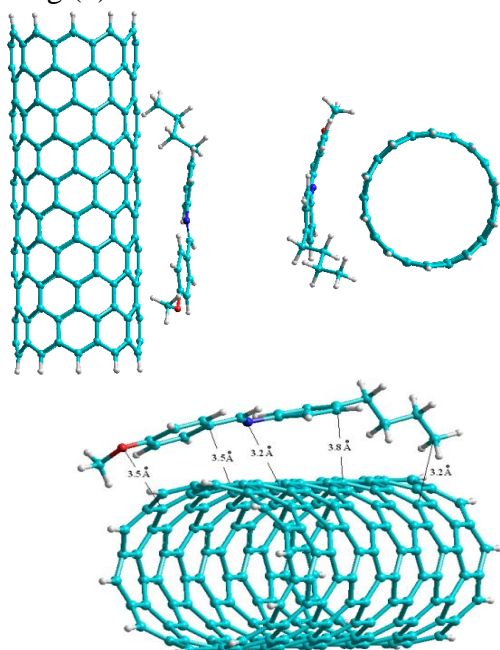


**Fig.(8) Side and top views of the MBBA molecule that assembly around the H-CNT. The distance is in angstrom between atoms of MBBA and nearest atoms of CNT molecules.**

Fig. (9) shows electrostatic potential energy maps of assembly CNT-MBBA model (-0.09 to + 0.18 in unit (e/atom), that illustrates electronic density distribution over the surface area of CNT molecule.

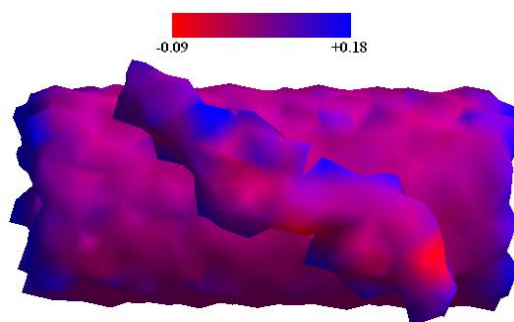


**Fig. (9) The electrostatic potential energy maps of assembly CNT- MBBA model.**

Although our calculations were limited by the short CNT length with symmetric functionalization at both edges, this provided some intuitive pictures for the formation of a permanent dipole moment. In a real situation, the tube diameters of the single-walled CNTs were usually in the range of 1-2 nm with a length of a few micrometers. The dispersion of the CNTs in LC medium resulted in assembly of several LC molecules along both the circumferential directions and the tube axis. The induced charge distribution in the CNTs was inevitably asymmetric, therefore producing net charges in the CNT and the permanent dipole moment. The magnitude of the dipole moment will be higher because of the long CNTs [23].

This large permanent dipole moment can be easily rotated at particularly high external voltage. The presence of a permanent dipole moment in the CNT resulting from the charge transfer from LC molecule can explain the simple translational motion of CNT under dc bias and its dynamical motion at ac bias with a critical field strength, which was experimentally observed [23].

**Table (1)**  
**Energetic parameters and frontier orbital energies (HOMO, LUMO), dipole moment ( $\mu$ ) of assembly models and their components calculated from the PM3 method.**

Molecule	Total energy (kcal/mol)	Binding energy (cal/mol)	Heat of formation (kcal/mol)	Dipole moment (D)	HOMO (eV)	LUMO (eV)	Gap <sup>a</sup> energy (eV)
MBBA	-67145.55	-	6.77	2.32	-8.6082	-0.6159	7.9923
H-T	-134298.34	-7.24	6.32	4.05	-8.5600	-0.5803	7.9797
H-H	-134296.61	-5.51	8.05	0.21	-8.5476	-0.5712	7.9764
CNT	-552867.43	-	1397.16	8.20	-5.4606	-4.2193	1.3313
MBBA-CNT	-610006.38	6.25	1418.19	2.63	-5.4438	-4.2329	1.1209

Gap<sup>a</sup> energy=LUMO-HOMO.

**Table (2)**  
**Mulliken charge distribution on MBBA molecule and MBBA-CNT model.**

Atoms	Mulliken charge (e), MBBA-CNT	Mulliken charge (e), MBBA
N	-0.07	-0.06
O	-0.19	-0.18
C <sub>3</sub>	-0.05	-0.02
C <sub>6</sub>	-0.07	-0.12
C <sub>end tail</sub>	-0.12	-0.11

## Conclusions

We searched for stable geometries of a LC molecule assembled on the CNT wall by means of semi-empirical molecular quantum calculations under PM3 method within hyperchem main frame. The  $\pi,\pi$ -stacking between MBBA molecule and these on the CNT wall led to anchoring of LC molecule on the CNT wall. The binding energy of the LC molecule on the CNT wall was within the typical van der Waals interaction. This binding originated from the electrostatic energy by a significant amount of charge transfer from the LC molecule to the CNT. Further calculations of the permanent dipole moment of the CNT could explain the dynamical motion of CNTs under various external fields.

## References

- [1] Stewart ,Optimization of Parameters for Semiempirical Methods I. Method, J. Comp. Chem., vol. 10, pp. 209, 1989.
- [2] Sarman S, Molecular dynamics simulation of thermomechanical coupling in cholesteric liquid crystals, Mol. Phys., vol. 98, pp. 27, 2000.
- [3] Tiwari S. N., Mishra M. and Sanyal N., Theoretical study of molecular ordering in p-n-hexyloxybenzylidene-p-toluidine, Indian J. Phys., vol. 76 B, pp. 17, 2002.
- [4] Mishra M, Dwivedi M K, Shukla R and Tiwari S N, Odd-even effect in p-alkyl-p'-cyanobiphenyl liquid crystalline series: An ab initio study, Prog. Cryst. Growth Charact. Mater, USA, vol. 114, pp. 52, 2006.
- [5] N. Tiwari, M Mishra and N. Sanyal, Theoretical study of molecular ordering in p-n-hexyloxybenzylidene-p-toluidine: A nematic liquid crystal, Indian J. Phys., vol. 45, pp. 83-88, January 2007.
- [6] Manuel V. García, Natalia H. Salazar, Antonio M. Richa and Juvencio Robles, Theoretical study of the experimental

- behavior of two homologous series of liquid crystals, ARKIVOC (xi), pp. 149-162, 2003.
- [7] M. Parra, J. Alderete, C. Zúñiga and S. Hernández, Synthesis, mesomorphic properties and structural study by semi-empirical calculations of amides containing the 1,3,4-thiadiazole unit, *Liq. Cryst.*, vol. 29, pp. 647-652.
- [8] Zhang Ran, He Jun, Peng Zeng-Hui and Xuan Li, Calculating the dielectric anisotropy of nematic liquid crystals: a reinvestigation of the Maier–Meier theory, *Chinese Phys. B* vol.18, pp. 2885, 2009.
- [9] Mayumi Goto, Tokifumi Masukawa, Tomoyuki Kondo and Atsuko Fujita, Novel Nematic Liquid Crystalline Compounds Having A Tetrahydropyran Ring, *Mol. Cryst. Liq. Cryst.*, vol. 494, pp. 58-67, 2008.
- [10] Lee, W.; Gau, J.-S.; Chen, H.-Y., Suppression of field screening in nematic liquid crystals by carbon nanotubes, *Appl. Phys.*, vol. B 81, pp. 171, 2005.
- [11] Huang, C.-Y.; Hu, C.-Y.; Pan, H.-C.; Lo, K.-Y. *Jpn.*, Impact of nanoscale particles and carbon nanotubes on current and future generations of liquid crystal displays, *J. Appl. Phys.*, vol. 44, pp. 8077, 2005.
- [12] I. Dierking, G. Scalia and P. Morales, Liquid crystal–carbon nanotube dispersions, *J. Appl. Phys.* vol. 97, pp. 044309, 2005.
- [13] J. Lagerwall, G. Scalia, M Haluska, U. Dettlaff-Weglikowska, S. Roth, F. Giesselmann, Nanotube alignment using lyotropic liquid crystals, *Adv. Mater.* vol. 19, pp. 359, 2007.
- [14] In-Su Baik, S. Y. Jeon, S. H. Lee, K. A. Park, S. H. Jeong, K. H. An, and Y. H. Lee, Nanoparticles-induced vertical alignment in liquid crystal cell, *Appl. Phys. Lett.*, vol. 87, pp.263110, 2005.
- [15] K. A. Park, S. M. Lee, S. H. Lee, and Y. H. Lee, Anchoring a liquid crystal molecule on a single-walled carbon nanotube, *J. Phys. Chem.*, vol. 111, pp.1620, 2007.
- [16] Rajratan Basu and Germano S. Iannacchione, Orientational coupling enhancement in a carbon nanotube dispersed liquid crystal, *phys. Rev.*, E vol. 81, pp. 051705, 2010.
- [17] M. D. Lynch and D. L. Patrick, Organizing Carbon Nanotubes with Liquid Crystals, *Nano Letters*, vol. 2, pp.1197, 2002.
- [18] HyperChem (TM) Professional 7.52, Hypercube, Inc., 1115 NW 4th Street, Gainesville, Florida 32601, USA, 2002.
- [19] T. Tsuji, H. Takashima, H. Takeuchi, T. Egawa, S. Konaka, Molecular structure of trans-azoxybenzene determined by gas electron diffraction combined with ab initio calculations, *J. of Molecular Structure*, vol. 554, pp. 203-210, 2000.
- [20] De Gennes, P. G.; Prost, J. *The Physics of Liquid Crystals*, 2<sup>nd</sup> ed.; Clarendon Press, Oxford, 1993.
- [21] Atkins, Peter and Julio de Paula. *Physical Chemistry for the Life Sciences*, Oxford, UK: Oxford University Press. 2006.
- [22] Tasis, D.; Tagmatarchis, N.; Bianco, A.; Praton, M. Aligned carbon nanotubes in the supramolecular order of discotic liquid crystals, *Chem. Rev.*, vol. 106, pp.1105, 2006.
- [23] Baik, I.-S.; Jeon, S. Y.; Jeong, S. J.; Lee, S. H.; An, K. H.; Jeong, S. H.; Lee, Y. H., Electroactive superelongation of carbon nanotube aggregates in liquid crystal medium, *J. Appl. Phys.*, vol. 100, pp. 074306, 2006.

#### الخلاصة

تمت الدراسة النظرية لاستقرارية الشكل الفراغي لجزيئات البلورات السائلة النيماتية (الخطية) المحتشدة على جدران الكربون النانوتيوب، باستخدام حسابات ميكانيك الكم التجريبية PM3 ضمن برنامج Hyperchem. وجد ان الاحتشاد ينتج من تأثير نوع  $(\pi, \pi)$  بين جزيئات MBBA الكربون النانوتيوب مؤدية الى تكوين طاقة الارتباط لمواقع قصيرة المدى تترتب فيها جزيئات البلورات السائلة ترتيباً اتجاهياً على جدار الانبوب النانوي. ان طبيعة التأثير المولد لطاقة الارتباط بين MBBA و CNT هي قوى فاندرفال و التي تنتج من التأثير الالكتروستاتيكي المتسبب من انتقال الشحنة من البلورات السائلة الى CNT .